

Acid-Induced Decomposition of Di-*tert*-butyl Peroxide in *n*-Heptane Solution up to High Temperatures and Pressures

By Michael Buback* and Lars Wittkowski

Institut für Physikalische Chemie, Universität Göttingen,
Tammannstraße 6, 37077 Göttingen, Germany

(Received January 16, 1998; accepted May 5, 1998)

Peroxides / Decomposition kinetics / High pressure / Methacrylic acid polymerization

The decomposition of di-*tert*-butyl peroxide (DTBP) in *n*-heptane with varying amounts of pivalic acid (PA) being added was studied via online FT-IR spectroscopy at elevated temperatures, 180 to 200°C, and pressures up to 2000 bar. A pronounced acid-induced DTBP decomposition is found without any PA consumption. Decomposition rates are adequately described by first-order kinetics. The pressure and the temperature dependence of acid-induced decomposition are investigated. The data suggest that the rate enhancement is due to the formation of a DTBP-PA complex. The acid-induced DTBP decomposition yields the same products as does the non-induced process (without acid being present). It thus appears justified to use the rate data observed for the model system DTBP-PA-*n*-heptane for the simulation of initiation rates in technical polymerizations where DTBP acts as the initiator and where acid is present, e.g. as a monomeric species.

Die Kinetik des Zerfalls von Ditertiärbutylperoxid (DTBP) in *n*-Heptan-Lösung wird bei Zugabe unterschiedlicher Mengen an Pivalinsäure (PA) bei erhöhten Temperaturen, zwischen 180 und 200°C, und Drücken bis 2000 bar durch quantitative Infrarotspektroskopie unter Meßbedingungen studiert. Es wird ein ausgeprägter säureinduzierter Zerfall des DTBP beobachtet, wobei sich die Säurekonzentration im Verlauf einer Zerfallsreaktion nicht verändert. Die Reaktion läßt sich jeweils durch ein Geschwindigkeitsgesetz 1. Ordnung beschreiben. Die Druck- und die Temperaturabhängigkeit des säureinduzierten DTBP-Zerfalls werden untersucht. Die wesentliche Ursache des beschleunigten Zerfalls wird in der Bildung eines DTBP-PA-Komplexes gesehen. Der säureinduzierte DTBP-Zerfall führt zu denselben Produkten wie der nicht-induzierte, ohne Säure erfolgende Zerfall. Es erscheint somit gerechtfertigt, die am Modellsystem erhaltenen kinetischen Daten zur Simulation technischer Polymerisationen mit DTBP als Initiator bei Anwesenheit von Säure zu nutzen, etwa bei Polymerisationen von Säuremonomeren.

1. Introduction

Organic peroxides are extensively used as initiators in free-radical polymerizations [1]. To model such processes, precise decomposition rate coefficients are required. As peroxide decomposition is not that easily measured during the course of a polymerization reaction, decomposition rates have been determined in a variety of non-polymerizable solvents [2]. Using on-line Fourier-transform IR spectroscopy, several diacyl peroxides [3] and peroxyesters [4] have been studied in *n*-heptane over an extended temperature range and up to pressures of a few kbar as are used in high-pressure ethene polymerization. To mimic situations that are found in the high-pressure free-radical polymerization of polar monomers or in copolymerizations where at least one monomer has a significant polarity, peroxide decomposition kinetics at high pressure has also been studied in solutions of toluene, chlorobenzene, chloroform, dichloromethane, propionitrile, and acetonitrile [5]. These investigations showed that the first-order decomposition rate coefficients of diacyl peroxides increase by almost one order of magnitude in going from a hydrocarbon solvent to acetonitrile.

It appears worthwhile to study whether added carboxylic acid influences peroxide decomposition in an unpolar solvent to the same or perhaps to an even larger extent than the above-mentioned polar materials. Investigations into acid-induced peroxide decomposition have already been carried out on peroxyesters and diacyl peroxides at ambient pressure [6–9] and significant rate enhancements have been observed. For a detailed understanding of such effects it appears reasonable to investigate the acid-induced decomposition of di-*tert*-butyl peroxide (DTBP) which may be looked upon as the basic technically relevant peroxide component.

The interest in acid-induced peroxide decomposition arises as in several free-radical copolymerizations, e.g. of ethene with (meth)acrylic acid, COOH groups are necessarily present. The ethene-(meth)acrylic acid copolymerizations are of considerable scientific and technical interest. They are carried out at fairly high pressures and temperatures, close to conditions used in ethene high-pressure homopolymerization. For this reason, the investigations into peroxide decomposition with acid being present also need to be performed at high pressures and temperatures. We decided to study the decomposition of di-*tert*-butyl peroxide (DTBP) in *n*-heptane with different amounts of pivalic acid (2,2-dimethylpropionic acid) being added.

DTBP is the classical example of a peroxide showing simple homolytic single bond scission and a large body of literature exists on DTBP decomposition [10–18]. The decomposition of DTBP at ambient pressure has already been studied in a wide variety of solvents, such as cyclohexane, triethylamine, dimethylaniline, cyclohexene, tetrahydrofuran, *t*-amyl alcohol, nitrobenzene, *t*-butyl alcohol, acetonitrile, and acetic acid by Huyser

and Van Scoy [10]. The first-order rate coefficients, k_{obs} , measured by these authors at temperatures between 115 and 135°C are rather similar. At 135°C these numbers agree with k_{obs} for *n*-heptane solution within a factor of two. Extrapolation of k_{obs} values measured in the various solvents, including *n*-heptane, to temperatures around 170°C yields almost identical numbers. No significant variation of k_{obs} with solvent polarity, say by more than 50 per cent, is expected for the 180 to 200°C range even upon major changes in molecular environment, e.g. in changing solvent from (pure) cyclohexane to acetonitrile and to (pure) acetic acid. This finding is consistent with rate studies performed on DTBP decomposition in acetonitrile at significant variation of pressure and temperature [11], where, e.g. for 500 bar and 180°C, an enhancement of k_{obs} by (only) 40 per cent compared to k_{obs} measured in *n*-heptane [12] has been found.

The kinetics of DTBP decomposition at pressures up to 2 kbar and up to 200°C has already been determined in (pure) *n*-heptane [11]. In the study presented here, the influence of pivalic acid on DTBP decomposition in *n*-heptane is also measured via quantitative FT-IR spectroscopy up to 2 kbar and 200°C.

2. Experimental

The decomposition kinetics were measured in a batch-type stainless steel (W.St.-Nr. 1.4122) autoclave equipped with two windows made from polycrystalline silicon. The cell for operation up to 200°C and 2000 bar has already been described [12]. At the relevant reaction temperatures above 150°C, the peroxide decomposition proceeds too fast as to allow for introducing the sample solution into the autoclave at ambient conditions and heating the cell, within several minutes, to the desired temperature. To avoid the problem of having the peroxide mostly decomposed before the desired reaction temperature is reached, only the evacuated optical cell is heated to the reaction temperature. The sample solution is pre-compressed, up to a maximum pressure of 3 kbar, in the pressure-generating part of the experimental set-up maintained at room temperature, where decomposition rate is sufficiently low to prevent any reaction even within extended storage times. After reaching the reaction temperature in the optical high-pressure cell, a valve between the cell and the pressure-generating system is opened. It takes about 5 to 10 seconds until the desired reaction conditions of p and T are reached within the cell. This time period includes fine tuning of the pressure to a desired value.

The pressure generator, gauges, valves and the capillaries are standard equipment. Pressure was measured by a DMS transducer (HBM-Meßtechnik, Class 2, maximum pressure 3 kbar). Temperature was recorded with a

sheathed thermocouple (Ni/Cr-Ni, CIA S250, CGA Alsthom) and controlled by a PID instrument (Eurotherm 820). The accuracy in pressure and temperature determination is ± 6 bar and $\pm 0.25^\circ\text{C}$, respectively.

Collection of spectral data was started immediately after reaching constant pressure and temperature conditions in the optical high-pressure cell. The spectra were recorded on a Bruker IFS 88 FT-IR/NIR spectrometer using a halogen source, a CaF_2 beam splitter, and a liquid-nitrogen-cooled InSb detector. For the experiments with methacrylic acid being present a nitrogen-cooled MCT detector was used. To speed up spectral data collection, only the interferograms were recorded (and stored) during the decomposition reaction. Fourier transformation and calculation of absorbance spectra from these data was performed after completion of the reaction. The IR spectrum measured on the evacuated cell at reaction temperature served as the reference spectrum.

Peroxide solutions were prepared in quantities of about 100 ml. Prior to the experiment, the solution was degassed by four freeze and thaw cycles. The DTBP concentration was close to 0.15 mol/kg heptane in all experiments with the amount of each component being measured with an accuracy of ± 0.001 g. Pivalic acid (PA) was added to the solutions to yield PA concentrations up to 0.178 mol/kg heptane. In one series of experiments methacrylic acid was added to the DTBP/heptane solution. The materials used in the reactions were: DTBP (>98%, Merck), pivalic acid (99.5%, Fluka), *t*-butanol (>99.5%, Merck), methacrylic acid (99.5%, Fluka), and *n*-heptane (>99%, Merck).

3. Results

In Fig. 1 is shown an absorbance spectral series measured at 200°C and 500 bar during the decomposition of DTBP in *n*-heptane with pivalic acid being added to yield a concentration of 0.122 mol PA/kg heptane. The initial peroxide concentration was 0.15 mol DTBP/kg heptane. The absorbance between 3600 and 3650 cm^{-1} , which increases during reaction, is due to *t*-butanol (TB). This product is formed in H-abstraction reactions of the intermediate *t*-butoxy radicals. The other major products are acetone (AC) and methane. They originate from the β -scission reaction of *t*-butoxy radicals which directly yields AC and leads to CH_4 formation by H-abstraction of the produced methyl radicals. The band at 3550 cm^{-1} is due to the absorbance of the PA monomer. No change in this acid absorbance is found during the decomposition reaction.

Independent spectroscopic experiments on solutions containing varying amounts of TB and of PA (at similar concentrations as used within the kinetic experiments) showed that Beer-Lambert's law holds for the PA

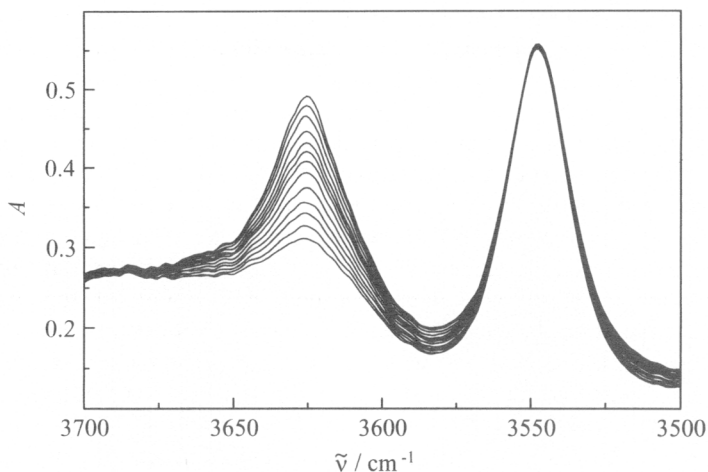


Fig. 1. Hydroxyl region of the infrared absorbance spectra collected during the decomposition of DTBP (0.15 mol/kg heptane) at 200°C and 500 bar in the presence of pivalic acid (0.122 mol/kg heptane). The *t*-butanol (TB) band around 3625 cm⁻¹ increases during decomposition whereas the acid absorption around 3550 cm⁻¹ remains constant.

monomer band at 3550 cm⁻¹ and for the TB band around 3630 cm⁻¹ in *n*-heptane solution at the *p* and *T* conditions of this work [19]. This information together with the observation of an almost invariant absorbance of the 3550 cm⁻¹ band in the kinetic experiment (Fig. 1) indicates that the PA concentration stays constant during the course of the decomposition reaction. Also within the other experiments, carried out at temperatures of 180, 190 and 200°C and at pressures between 100 and 1900 bar, no indication of any change in PA concentration is provided by the absorbance around 3550 cm⁻¹. Thus it appears reasonable to use a first-order rate law [Eq. (1)] for fitting the DTBP concentration during both the decomposition in *n*-heptane solution containing some PA and for the decomposition without acid being present:

$$\frac{dc_{\text{DTBP}}}{dt} = -k_{\text{obs}} \cdot c_{\text{DTBP}} \quad (1)$$

Tertiary butanol (TB) and acetone (AC) are the only oxygen containing products that are identified from IR and GC analysis in the samples of this study. Assuming TB and AC to be produced by parallel first-order reactions, characterized by rate coefficients k_{TB} and k_{AC} , respectively, allows to derive Eq. (2). By assuming that the fraction of DTBP that reacts to TB,

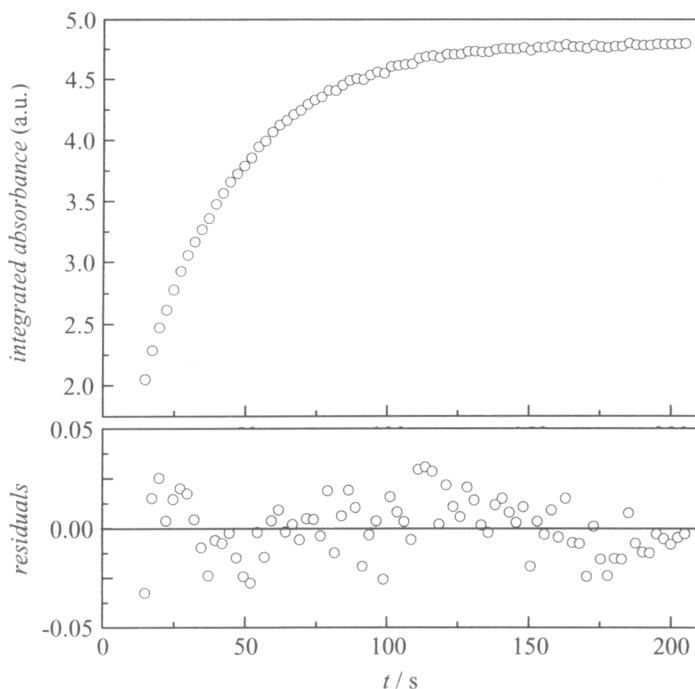


Fig. 2. Upper part: Integrated absorbance of the OH stretching mode of TB (see text) measured as a function of reaction time t during the decomposition of DTBP in n -heptane at 200°C and 500 bar at an acid concentration of 0.122 mol/kg heptane. The initial DTBP concentration was 0.15 mol/kg heptane. Lower part: residuals with respect to the curve fitted by Eq. (2).

$k_{\text{TB}}/(k_{\text{TB}} + k_{\text{AC}})$, stays constant during a particular DTBP decomposition reaction, even without knowing a number for this ratio, k_{obs} is directly accessible from the spectroscopically measured TB concentration, c_{TB} , via Eq. (2).

$$c_{\text{TB}} = c_{\text{TB}}^{\infty} - 2 c_{\text{DTBP}}^0 \frac{k_{\text{TB}}}{k_{\text{TB}} + k_{\text{AC}}} \cdot \exp \{-k_{\text{obs}} \cdot t\}. \quad (2)$$

In Eq. (2), c_{TB}^{∞} and c_{DTBP}^0 refer to TB concentration after complete decomposition and to the initial DTBP concentration, respectively. The overall decomposition rate coefficient, k_{obs} , is found by non-linear regression (using the Levenberg-Marquard algorithm) of the spectroscopically measured TB concentration vs. time data. Within this fitting procedure the TB concentration, c_{TB} , is replaced by the TB absorbance integrated between 3620 and 3645 cm^{-1} against a horizontal baseline defined by the absorbance at 3720 cm^{-1} (not shown in Fig. 1). An important advantage of the non-linear

Table 1. Overall rate coefficient k_{obs} for the decomposition of DTBP in *n*-heptane at different pivalic acid concentrations, temperatures, and pressures. The initial peroxide concentration was 0.15 mol/kg heptane; ⁽¹⁾ rate coefficients derived from a fit of the literature data for 500 bar and temperatures from 140 to 200°C; ⁽²⁾ rate coefficients derived from a fit of the literature data for 190°C at pressures from 100 to 2000 bar. (*) Rate coefficients deduced from Ref. [12], according to procedures ⁽¹⁾ or ⁽²⁾.

| c_{PA} mol/kg heptane | $k_{\text{obs}} \cdot 10^3/\text{s}^{-1}$ at 500 bar | | |
|-----------------------------------|--|--------|--------|
| | 180°C | 190°C | 200°C |
| 0 ⁽¹⁾ | 4.22 * | 10.0 * | 23.0 * |
| 0 | 4.12 | 9.63 | 22.0 |
| 0.029 | 4.67 | 9.76 | |
| 0.033 | 5.16 | 11.2 | 23.7 |
| 0.078 | 7.09 | 14.7 | 28.8 |
| 0.122 | 9.42 | 15.4 | 28.9 |
| 0.167 | 9.92 | 18.2 | 33.8 |
| 0.178 | 9.98 | 16.5 | 31.4 |

| c_{PA} mol/kg heptane | $k_{\text{obs}} \cdot 10^3/\text{s}^{-1}$ at 190°C | | | | |
|-----------------------------------|--|---------|----------|----------|----------|
| | 100 bar | 500 bar | 1000 bar | 1500 bar | 1900 bar |
| 0 ⁽²⁾ | 11.1 * | 10.3 * | 9.2 * | 8.2 * | 7.6 * |
| 0.033 | 11.8 | 11.2 | 10.1 | 9.55 | 9.11 |
| 0.119 | 14.9 | 14.6 | 14.0 | 13.7 | 14.1 |
| 0.178 | 15.1 | 16.5 | 16.2 | 16.4 | 15.4 |

regression relates to the fact that a constant absorbance background, e.g. due to solvent absorbance is considered in the fitting procedure [19], and therefore does not interfere the analysis for k_{obs} .

Applying this kind of analysis to the decomposition reaction depicted in Fig. 1 yields the TB absorbance vs. time plot shown in the upper part of Fig. 2. Each data point is derived from an independent spectroscopic measurement. The number of data points in Fig. 2 largely exceeds the number of spectra shown in Fig. 1. This is because only a fraction of the actually measured spectra has been plotted. In the lower part of Fig. 2 the difference between measured and fitted [by Eq. (2)] absorbance is presented. This plot of residuals demonstrates the adequate representation of kinetic data by the first-order rate law [Eqs. (1) and (2)].

Analysis of the spectroscopic data measured during the course of DTBP decomposition at the other temperatures, pressures, and PA concentrations shows the same type of behaviour. The first-order rate coefficients, k_{obs} , derived from analysis via Eq. (2), are given in Table 1.

The accuracy of k_{obs} values is estimated to be better than ± 10 per cent. Included in Table 1 are the k_{obs} values from the earlier study of DTBP de-

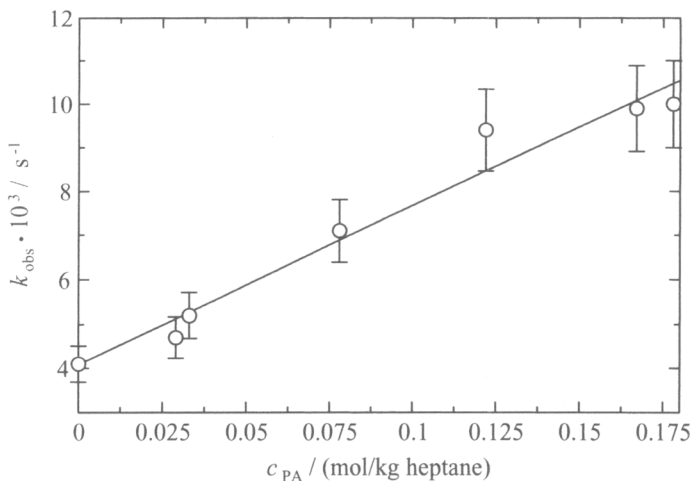


Fig. 3. Dependence on pivalic acid concentration (c_{PA}) of the observed rate coefficient (k_{obs}) for DTBP decompositions in *n*-heptane at 180°C and 500 bar. The error bars correspond to an uncertainty of $\pm 10\%$.

composition in (pure) *n*-heptane [12]. These data (at $c_{PA} = 0$) are marked with an asterisk. Within the present work only three such data points (at $c_{PA} = 0$) have been measured: at 500 bar and 180, 190, and 200°C. The numbers are in very pleasing agreement with the literature data.

As can be seen from Table 1, k_{obs} is significantly enhanced toward higher temperature. The influence of pressure is less pronounced. At low levels of c_{PA} , pressure lowers k_{obs} whereas at the higher PA concentrations no clear trends can be seen.

Plotted in Fig. 3 is the dependence of k_{obs} on PA concentration for DTBP decompositions carried out at 180°C and 500 bar. Within an uncertainty of ± 10 per cent, represented by the error bars, the k_{obs} values may be fitted by a straight line. As is indicated by a very few experiments at PA concentrations exceeding 0.178 mol/kg of *n*-heptane, k_{obs} does not continue to linearly increase with c_{PA} at such higher PA concentrations. A closer look at the data in Fig. 3 and in Table 1 indicates that for $c_{PA} > 0.1$ mol PA/kg heptane the increase in k_{obs} is less pronounced and, within experimental uncertainty, no clear enhancement of k_{obs} upon the addition of further PA is seen. Nevertheless it appears justified to fit the k_{obs} vs. c_{PA} data at concentrations up to 0.178 mol PA/kg heptane by a linear relation. In doing so, for each of the experimental decomposition studies carried out at constant p and T , a correlation of the quality as shown in Fig. 3 is achieved.

4. Discussion

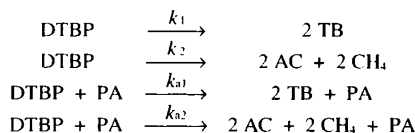
Investigations into peroxide decomposition are of both mechanistic and practical interest, the latter being due to the widespread use of these materials as initiators in free-radical homo- and copolymerizations. As the monomers may influence the reactivity and selectivity of peroxide decomposition through their polarity or even by a direct participation in the decomposition process, detailed studies into the peroxide decomposition kinetics at considerable variation of molecular environment, by changing solvent type, solvent concentration, pressure, and temperature are required. Particularly strong effects on decomposition rate are expected to occur when COOH groups are present. The practical interest in such systems is due to acrylic and methacrylic acid being important (co)monomers. The present study focuses on DTBP decomposition in solution of *n*-heptane with different amounts of pivalic acid (PA) being added to mimic situations as occur in ethene-(meth)acrylic acid copolymerizations. As these technical reactions are carried out at high pressures and temperatures, also our studies are performed within an extended p and T range.

The decomposition kinetics of DTBP in (pure) *n*-heptane has already been measured [12]. A few such experiments have also been carried out in the present investigation (see Table 1). It is gratifying to note that, within an experimental uncertainty of ± 10 per cent, excellent agreement is found with the numbers from the earlier study (where comparison with the entire body of existing literature has been made).

As can be seen from Fig. 3 and from the entries in Table 1, the observed first-order rate coefficient, k_{obs} , is significantly enhanced upon the addition of pivalic acid, in particular at concentrations up to $c_{\text{PA}} = 0.1$ mol/kg heptane. The spectroscopically measured decomposition product is *t*-butanol. Acetone (AC) is also formed but it is only in the absence of PA or at very low levels of PA easily identified via the carbonyl stretching mode at around 1720 cm^{-1} [4]. Acetone is produced by a β -scission reaction of intermediate *t*-butoxy radicals. Thus methane produced by H-abstraction of the methyl radicals (from this β -scission) will be another product. In solution of *n*-heptane these small amounts of methane may, however, not be detected via online IR spectroscopy.

The kinetic observations may be represented by Scheme 1 which applies to both decomposition in the absence and in the presence of PA:

It should be noted that the individual reactions in Scheme 1 are not balanced for hydrogen (which is picked up from the solvent). The observations going into Scheme 1 are: (i) TB and AC are the only oxygen-containing products that are seen in the spectra. Gas-chromatographic analysis indicates that no other oxygen-containing products are formed in quantities above 0.1 per cent relative to decomposed peroxide; (ii) TB and AC occur with and without PA being present; (iii) The concentration of



Scheme 1. Scheme for the decomposition of DTBP in *n*-heptane with PA being present. Reaction channels are not balanced with respect to the amount of hydrogen (see text).

pivalic acid does not vary during the course of a decomposition reaction up to complete DTBP conversion. Thus PA is added on both sides of the third and fourth equation in Scheme 1.

The relation between these individual coefficients and the experimentally measured quantity k_{obs} is: $k_1 + k_2 + k_{a1} \cdot c_{\text{PA}} + k_{a2} \cdot c_{\text{PA}} = k_{\text{obs}}$. As the individual reaction pathways yielding TB and AC cannot be distinguished within the experiments of the present study, the following substitution is made:

$$k_1 + k_2 = k_{\text{HE}}, \quad (3)$$

$$k_{a1} + k_{a2} = k_{\text{PA}}. \quad (4)$$

As a consequence, the observed overall rate coefficient k_{obs} may be represented by:

$$k_{\text{obs}} = k_{\text{HE}} + k_{\text{PA}} \cdot c_{\text{PA}} \quad (5)$$

where k_{HE} refers to the first-order rate coefficient of DTBP decomposition in *n*-heptane and k_{PA} to the second-order rate coefficient of (pivalic)acid-induced decomposition. It should be noted that, because of c_{PA} remaining constant during each decomposition reaction, the product term in Eq. (5), $k_{\text{PA}} \cdot c_{\text{PA}}$, may be looked upon as a pseudo first-order rate coefficient.

From the fitted linear dependence of k_{obs} on c_{PA} , which has been shown for 500 bar and 180°C in Fig. 3, the rate coefficients k_{HE} and k_{PA} , according to Eq. (5), are available from the intersection with the ordinate and from the slope of the straight line, respectively. The k_{HE} and k_{PA} values derived by this procedure are given in Table 2 for three temperatures at constant pressure (500 bar) and for five pressures at constant temperature (190°C). The k_{HE} values increase with temperature and decrease with pressure. k_{PA} is enhanced toward higher temperature, too, but also increases with pressure, at least up to 1500 bar.

Shown in Fig. 4 is the temperature dependence of k_{HE} and of acid-induced decomposition, represented by the pseudo first-order rate coefficient $k_{\text{PA}} \cdot c_{\text{PA}}$ for the arbitrarily chosen concentration of $c_{\text{PA}} = 0.1 \text{ mol/kg}$ heptane. The activation energy of k_{HE} , $E_A(k_{\text{HE}})$, largely exceeds $E_A(k_{\text{PA}})$. The difference is visualized in plotting activation energy vs. pre-exponential factor, A , in Fig. 5. This diagram takes into account that both quantities are

Table 2. Rate coefficients of non-induced decomposition (k_{HE}) and induced decomposition (k_{PA}) of DTBP in *n*-heptane. Data are calculated via linear regression according to Eq. (5). The uncertainty in k_{HE} and k_{PA} is determined by the square root of the variance of the intercept and of the slope from linear regression.

| $T/^\circ\text{C}$ (at 500 bar) | $k_{HE} \cdot 10^3/\text{s}^{-1}$ | $k_{PA} \cdot 10^3/\text{kg s}^{-1} \text{mol}_{PA}^{-1}$ |
|---------------------------------|-----------------------------------|---|
| 180 | 4.1 ± 0.3 | 36 ± 3 |
| 190 | 9.6 ± 0.6 | 46 ± 6 |
| 200 | 22 ± 1 | 60 ± 9 |
| p/bar (at 190°C) | $k_{HE} \cdot 10^3/\text{s}^{-1}$ | $k_{PA} \cdot 10^3/\text{kg s}^{-1} \text{mol}_{PA}^{-1}$ |
| 100 | 11.3 ± 0.5 | 24 ± 5 |
| 500 | 10.2 ± 0.1 | 36 ± 3 |
| 1000 | 9.0 ± 0.2 | 41 ± 2 |
| 1500 | 8.1 ± 0.1 | 47 ± 1 |
| 1900 | 7.8 ± 0.6 | 46 ± 5 |

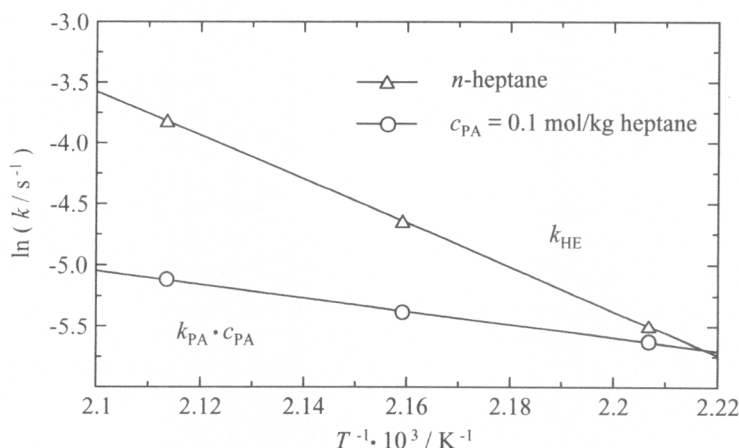


Fig. 4. Temperature dependence of acid-induced ($k_{PA} \cdot c_{PA}$) and non-induced (k_{HE}) decomposition of DTBP in *n*-heptane solution at 500 bar, $c_{PA} = 0.1 \text{ mol/kg}$ heptane.

highly correlated via the Arrhenius relation ($k = A \cdot \exp\{-E_A/(R \cdot T)\}$). Given in Fig. 5 are the joint confidence intervals (JCI's) referring to a confidence level of 95 per cent [20].

The JCI's in Fig. 5 are rather extended as a consequence of applying the F-distribution at a confidence level of 95 per cent to data at only three temperatures. Calculation of JCI's with the χ^2 -distribution and with the variance σ^2 of rate coefficients from Table 2 results in smaller ellipses. The

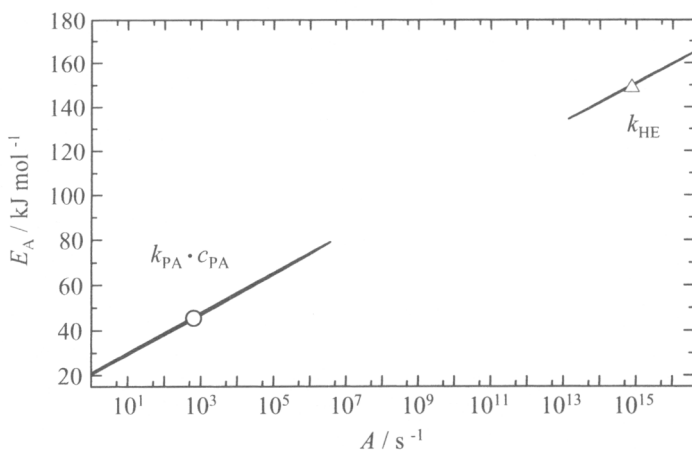


Fig. 5. 95% Joint confidence intervals of the Arrhenius parameters for acid-induced ($k_{PA} \cdot c_{PA}$) and non-induced (k_{HE}) decomposition of DTBP in *n*-heptane at 500 bar, $c_{PA} = 0.1$ mol/kg heptane.

Table 3. Overall activation energy E_A and corresponding frequency factor A for the decomposition of DTBP at 500 bar. Estimated uncertainties of E_A and A are determined from the difference between the outer limits of JCI's and the optimum values (see text).

| Reaction | System | A/s^{-1} | $E_A/kJ\ mol^{-1}$ |
|------------|--------------------------------------|---|--------------------|
| k_{HE} | <i>n</i> -heptane, PA | $7.5 \cdot 10^{14}$ ($+4 \cdot 10^{16}$, $-7 \cdot 10^{14}$) | 150 ± 15 |
| k_{HE}^0 | <i>n</i> -heptane | $6.7 \cdot 10^{14}$ ($+2 \cdot 10^{16}$, $-6.5 \cdot 10^{14}$) | 150 ± 14 |
| k_{HE}^0 | <i>n</i> -heptane ⁽¹⁾ | $1.2 \cdot 10^{15}$ ($+2 \cdot 10^{16}$, $-1 \cdot 10^{15}$) | 151 ± 11 |
| k_{PA} | <i>n</i> -heptane, PA ⁽²⁾ | $6.3 \cdot 10^3$ ($+3 \cdot 10^6$, $-6 \cdot 10^2$) | 46 ± 33 |

⁽¹⁾ Calculated from rate coefficients measured at 500 bar and temperatures between 140 and 200°C from Ref. [12].

⁽²⁾ Calculated for a PA concentration of 0.1 mol/kg heptane.

procedure of calculating the JCI's and of properly taking the error structure of the data sets into account, is described in quite some detail elsewhere [20].

Given in Table 3 are the activation energy and pre-exponential factor determined by means of non-linear regression for the decomposition of DTBP in *n*-heptane and for the corresponding (pivalic)acid-induced decomposition. As can be seen from Table 3, the activation energy and pre-exponential factor from data of Ref. [12] in (pure) *n*-heptane, from data in (pure) *n*-heptane of this work, and from the k_{HE} data of Table 2 are in excellent agreement. The JCI's of these three sets of data are nearly identical.

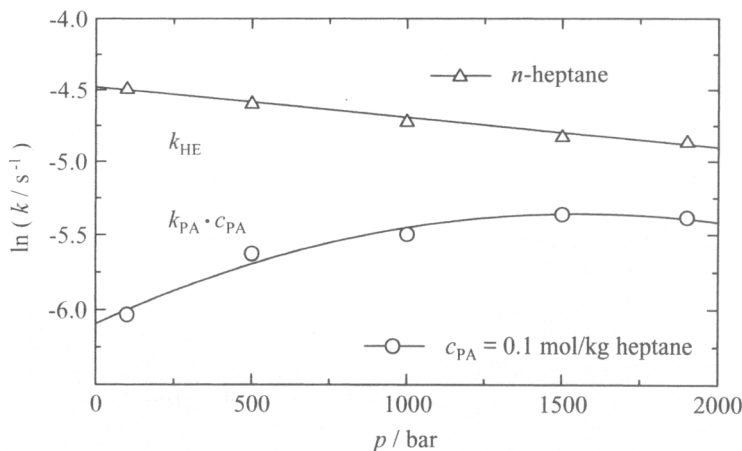


Fig. 6. Pressure dependence of the rate coefficients for acid-induced ($k_{PA} \cdot c_{PA}$) and non-induced (k_{HE}) decomposition of DTBP in *n*-heptane solution at 190°C, $c_{PA} = 0.1$ mol/kg heptane.

Analysis of the $k_{PA} \cdot c_{PA}$ values as a function of temperature leads to the very extended JCI depicted in Fig. 5 from which the activation energy of k_{PA} is deduced to be: $E_A(k_{PA}) = 46 \pm 33$ kJ mol⁻¹. In deriving this value it is assumed that the temperature dependence of $k_{PA} \cdot c_{PA}$ is entirely due to k_{PA} . Although the uncertainty in $E_A(k_{PA})$ is fairly large, this activation energy undoubtedly is far below $E_A(k_{HE})$, the activation energy for the non-induced process.

Before turning to the question why the two activation energies are so different, the pressure dependence of k_{HE} and of $k_{PA} \cdot c_{PA}$ (at $c_{PA} = 0.1$ mol/kg heptane) will be addressed. In Fig. 6 the rate coefficients for 190°C, from Table 2, are plotted vs. pressure.

The activation volume, $\Delta V^\ddagger = -RT(\partial \ln k / \partial p)_T$, for the non-induced decomposition is found to be: $\Delta V^\ddagger(k_{HE}) = 8.2 \pm 0.7$ cm³ mol⁻¹, in excellent agreement with $\Delta V^\ddagger(k_{HE}^0) = 8.5 \pm 0.7$ cm³ mol⁻¹ derived by applying the same fitting procedure to the data from Ref. [12].

The activation volume for k_{PA} is strikingly different, not only in absolute value but also in sign. Moreover, the $\ln(k_{PA} \cdot c_{PA})$ vs. p plot is curved which says that the formally derived activation volume depends on pressure. From the parabolic fit to the data, activation volumes $\Delta V^\ddagger(k_{PA})/\text{cm}^3 \text{ mol}^{-1}$ of: -37 at 1 bar, -25 at 500 bar and -14 at 1000 bar are calculated. The relatively large negative activation volumes at low pressure are close to values found in associative or bond-forming processes whereas the positive activation volumes, as observed for k_{HE} , are characteristic for bond-scission reactions and thus meet the expectations for a peroxide decomposition process.

What may be the reason(s) for the significant difference in decomposition rate of DTBP in *n*-heptane in the absence and in the presence of PA? There is no debate that decomposition in (pure) *n*-heptane proceeds via homolytic O–O bond scission yielding *t*-butoxy radicals within the primary kinetic step [13]. The measured values of pre-exponential factor, of activation energy, and of activation volume are fully consistent with this view. With acid being present, the reaction obviously does not follow a simple route. The following alternative reaction pathways may contribute or may become dominant in the presence of PA: (a) DTBP decomposes via an ionic mechanism; (b) There is an indirect influence in that acid reacts with the metal walls to produce metal ions that affect DTBP decomposition rate; (c) An induced free-radical reaction occurs with acid molecules participating in hydrogen transfer processes; (d) The polarity of the solvent medium is enhanced by the acid giving rise to an increase in k_{obs} ; (e) A specific association between DTBP and PA allows for a free-radical pathway associated with a much smaller activation energy.

The relevance of arguments (a) – (e) will now be discussed.

(a) Ionic mechanism

The low value of $E_{\text{A}}(k_{\text{PA}})$ provides some indication of an ionic mechanism. On the other hand, *n*-heptane is no overly suitable medium for an acid-catalyzed reaction to proceed. Moreover, a protonation reaction would yield an intermediate carbocation which must be expected to rearrange and yield 2-methoxypropene or react with a pivalic acid anion to form an ester. Thus an ionic mechanism should be accompanied by a major change in type and concentration of decomposition products. To see whether such changes occur, two decompositions of a 0.1 molar solution of DTBP in *n*-heptane, one with adding PA to yield a 1:1 molar ratio of DTBP to PA and one without acid, have been carried out under helium atmosphere in a sealed glass ampoule at 175°C. GC analysis of the liquid phase which contains more than 95% of the products yields the product distribution listed in Table 4. This GC analysis has been carried out at the Research Centre Deventer of Akzo Nobel. The gas phase which has also been analyzed contained the expected products: methane, ethane, acetone, and *t*-butanol.

The entries in Table 4 demonstrate that, within an accuracy of ± 10 per cent for the individual amounts and for the DTBP mass balance (sum of 0.5 times the acetone and *t*-butanol amounts and the amount of DTBP after reaction), the type and the concentration of products is not distinctly different for decompositions with and without pivalic acid. It should be noted that the significant concentration of C_7 -dimer, which proves the reaction of free radicals with the solvent *n*-heptane, unambiguously shows that radicals are the reactive species. For these reasons it can be ruled out that an ionic mechanism dominantly contributes to the acid-induced DTBP decomposition reaction.

Table 4. Liquid phase product distributions for the decomposition of DTBP in *n*-heptane at 175°C under He atmosphere with and without pivalic acid being present. Pivalic acid and initial DTBP concentrations were 0.1 M. The DTBP balance refers to the oxygen-containing species.

| Product | Product amount (mol/mol DTBP) | |
|-----------------------|-------------------------------|---------|
| | without PA | with PA |
| Acetone | 0.619 | 0.612 |
| <i>t</i> -Butanol | 1.272 | 1.184 |
| DTBP | 0.004 | 0.003 |
| C ₇ -dimer | 0.572 | 0.520 |
| DTBP-balance | 95.0% | 90.1% |

(b) Metal ion catalysis

As is well-known, metal ions may significantly enhance peroxide decomposition rates. For this reason the autoclave has been manufactured from a stainless steel which is poor in catalytically active metals. There are two other arguments why metal ion catalysis is not overly likely: (1) The reaction closely follows first-order kinetics which makes it hard to believe that the production of active (metal ion) species occurs in a way that affords for the observed simple first-order kinetics; and (2) as has been mentioned before, toward higher PA concentrations no further rate enhancement is found. It should finally be noted, that the major part of the internal reactor surface is polycrystalline silicon, the window material. Thus, although a contribution from metal ion catalysis cannot be excluded, such a mechanism can, at best, be of minor importance.

(c) Induced free-radical process

Induced processes where initiator is decomposed by a free-radical chain reaction are known to strongly contribute to hydroperoxide reactivity [13]. With no hydrogen atom in α -position to the O–O bond, however, DTBP is no obvious candidate for a significant contribution of induced decomposition. Moreover, pivalic acid has no particularly strong free-radical chain-transfer activity. If chain transfer would significantly contribute to acid-induced decomposition, the experimental observation (see introductory section) of DTBP decomposing at almost the same rate in cyclohexane and in pure acetic acid could hardly be understood. It thus appears unlikely that free-radical induced reactions are responsible for the observed acid-induced decomposition of DTBP.

(d) Solvent polarity

As has been shown by high-pressure studies on bis(3,5,5-trimethylhexanoyl)peroxide, solvent polarity may significantly vary decomposition rate, e.g. by a factor of 7 in going from *n*-heptane to acetonitrile. The solvent influence on DTBP decomposition seems to be much less as is indicated by the ambient pressure data of Huyser and VanScoy [10]. High-pressure studies into solvent dependence of DTBP decomposition are not available with the exception of a study by Drefahl, who measured DTBP decomposition in (pure) acetonitrile [11]. For 180°C and 500 bar he found $k_{\text{obs}} = 5.8 \cdot 10^{-3} \text{ s}^{-1}$ which is (only) by about 40 per cent above k_{HE} at the same *p* and *T* conditions. The corresponding value of the present investigation for $c_{\text{PA}} = 0.178 \text{ mol/kg}$ heptane is $9.98 \cdot 10^{-3} \text{ s}^{-1}$ which is by about 140 per cent above k_{HE} . As the k_{obs} value measured in the acid solution, where the ratio of PA to *n*-heptane molecules equals 1:600, is clearly above k_{obs} in the highly polar acetonitrile, it may be concluded that bulk solvent polarity is not responsible for the acid-induced enhancement observed for DTBP. At such low concentrations of PA relative to *n*-heptane also changes in transport coefficients are very unlikely to be of any relevance for acid-induced DTBP decomposition. It is for this reason that diffusion or viscosity effects will not be considered among the arguments that may account for the significant changes in k_{obs} .

(e) Specific association

The large negative activation volumes for k_{PA} , $\Delta V^{\ddagger}(k_{\text{PA}})$, suggest that an associative process significantly contributes to the acid-induced decomposition. The $\Delta V^{\ddagger}(k_{\text{PA}})$ value for ambient pressure ($-37 \text{ cm}^3 \cdot \text{mol}^{-1}$) is close to activation volumes measured for Diels-Alder reactions, which are assumed to occur via cyclic transition structures [21]. That carboxylic acids may form such cyclic structures is well-known from the existence of their hydrogen-bonded dimer species. The dimerization equilibrium of PA in dilute solution of *n*-heptane has already been studied in extended pressure and temperature ranges, up to 2000 bar and 175°C, respectively [22].

There is no direct evidence on the existence of DTBP-PA complexes, e.g. from the spectra measured during the course of the DTBP decomposition. If such complexes are formed, they will coexist with PA monomer and dimer species and thus will not be easily identified from the IR spectra. It should, however, be noted that various observations made for the PA-induced decomposition of DTBP are at least not in disagreement with postulating the existence of such DTBP-PA complexes. In addition to the argument about $\Delta V^{\ddagger}(k_{\text{PA}})$, also $E_{\text{A}}(k_{\text{PA}})$ may, at least qualitatively, be explained by DTBP-PA complexation. In case that such complexes are formed rapidly

as compared to their decomposition rate, k_d , the PA-induced rate coefficient k_{PA} is related to k_d and to K_C , the equilibrium constant for DTBP-PA complex formation, by Eq. (6):

$$k_{PA} = k_d \cdot K_C. \quad (6)$$

Introducing temperature dependences for k_d and K_C leads to:

$$E_A(k_{PA}) = E_A(k_d) + \Delta H_C \quad (7)$$

where ΔH_C is the complexation enthalpy. This value is not known for the postulated DTBP-PA species. The dimerization enthalpy of PA in *n*-heptane, $\Delta H_D = -50 \text{ kJ mol}^{-1}$, may serve as some reference value with the understanding that, in absolute values, ΔH_C will be lower than ΔH_D . Eq. (7) illustrates that $E_A(k_{PA})$ should be (significantly) below $E_A(k_d)$. Assuming that the activation energy for the decomposition into *t*-butoxy radicals of acid-complexed DTBP is smaller than $E_A(k_{HE})$, leads to an appreciable difference between $E_A(k_{PA})$ and $E_A(k_{HE})$. This is what is seen from the experimental data in Fig. 4.

Another argument in favour of the complexation hypothesis comes from the dependence of k_{obs} on PA concentration. Toward higher c_{PA} the PA dimer concentration is enhanced relative to the monomer concentration. As the PA dimer species are not available for complex formation, k_{obs} will not continue to linearly increase with c_{PA} as is observed for PA concentrations above 0.1 mol/kg solution.

The arguments on the origin of acid-induced enhancement of k_{obs} with c_{PA} may be summarized: A reaction which proceeds via a DTBP-PA complex that decomposes by producing *t*-butoxy radicals seems to provide the best explanation for all experimental findings. The pressure dependence (at 190°C) of k_{HE} and of $k_{PA} \cdot c_{PA}$ (at $c_{PA} = 0.1 \text{ mol/kg}$ heptane) may be represented by Eqs. (8) and (9), respectively, which have been deduced from the data in Table 2:

$$\ln(k_{HE}/s^{-1}) = -4.48 - 2.12 \cdot 10^{-4} (p/\text{bar}) \quad (\text{at } 190^\circ\text{C}) \quad (8)$$

$$\ln(k_{PA} \cdot c_{PA}/s^{-1}) = -6.06 + 9.5 \cdot 10^{-4} (p/\text{bar}) - 3.0 \cdot 10^{-7} (p/\text{bar})^2 \\ (\text{at } 190^\circ\text{C}, c_{PA} = 0.1 \text{ mol/kg}) \quad (9)$$

The temperature dependence (at 500 bar) of k_{HE} and $k_{PA} \cdot c_{PA}$ (at $c_{PA} = 0.1 \text{ mol/kg}$ heptane) is given by the Arrhenius expressions, Eqs. (10) and (11), respectively:

$$k_{HE}/s^{-1} = 7.5 \cdot 10^{14} \cdot \exp\{-18041/(T/K)\} \quad (\text{at } 500 \text{ bar}) \quad (10)$$

$$k_{PA} \cdot c_{PA}/s^{-1} = 6.3 \cdot 10^2 \cdot \exp\{-5533/(T/K)\} \\ (\text{at } 500 \text{ bar}, c_{PA} = 0.1 \text{ mol/kg}). \quad (11)$$

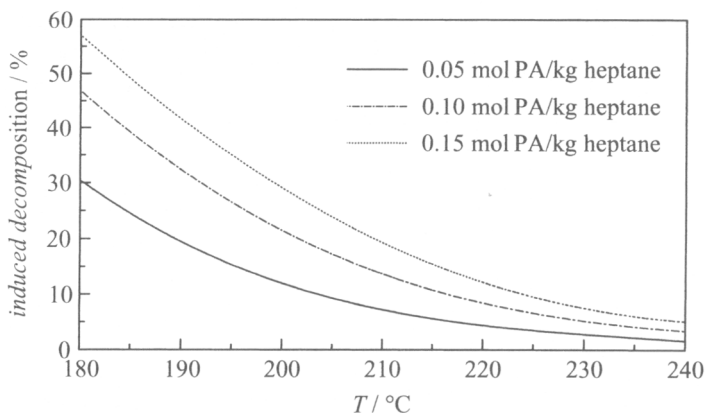


Fig. 7. Percentage of acid-induced decomposition to overall decomposition of DTBP in *n*-heptane as a function of temperature at 500 bar. The data are calculated from Eqs. (10) and (11) for three concentrations of monomeric PA, $c_{\text{PA}} = 0.05, 0.10,$ and 0.15 mol/kg heptane.

Using Eqs. (8)–(11) (where the concentration of PA refers to 0.1 mol per kg *n*-heptane) the fraction of acid-induced decomposition to overall decomposition, $k_{\text{PA}} \cdot c_{\text{PA}}/k_{\text{obs}}$, may be calculated. In Fig. 7 this fraction (in per cent) is plotted as a function of reaction temperature for PA-induced DTBP decompositions at 500 bar and three PA concentrations. The percentage of acid-induced decomposition increases with c_{PA} and significantly decreases with temperature. It should be noted that, according to the preceding discussion, c_{PA} refers to monomeric PA. Above 240°C, PA-induced decomposition contributes by less than 10 per cent to overall DTBP decomposition. This observation is of interest with respect to ethene-methacrylic acid copolymerizations which, in order to ensure homogeneity of the polymerizing system, are performed at such high temperatures.

It is beyond the scope of this paper to also measure DTBP decomposition during the course of an ethene-methacrylic acid copolymerization which is the technically relevant system behind the *n*-heptane/pivalic acid model system studied here. It is only one aspect of polymerizing (meth)acrylic acid with DTBP as the initiator that will be briefly addressed in this final section: The preceding discussion provides arguments for acid-induced decomposition being due to monomeric acid. If the acid is a monomer component, as is the case with (meth)acrylic acid, the question has to be asked whether the polymerized acid segments, which may be largely engaged in intramolecular association, also give rise to acid-induced peroxide decomposition.

To give an answer, the model system has been changed from DTBP/*n*-heptane/PA to DTBP/*n*-heptane/methacrylic acid (MAA). The polymeriza-

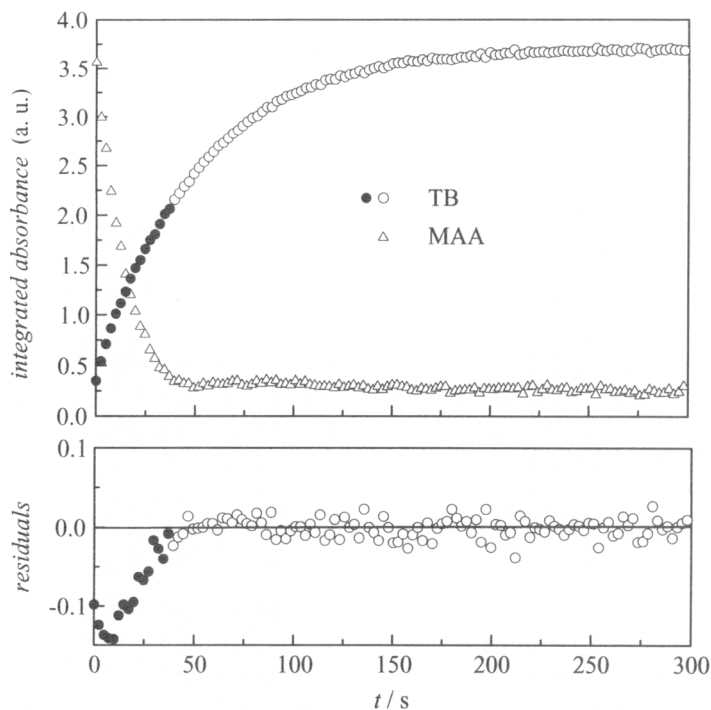


Fig. 8. Time evolution of TB and MAA concentration (represented by their characteristic IR absorbance) during a DTBP decomposition in *n*-heptane at 200 °C and 500 bar. The initial MAA and DTBP concentrations were 0.160 mol/kg heptane and 0.150 mol/kg heptane, respectively. Only the TB concentrations (integrated absorbances) represented by open symbols were subjected to a first-order fit for k_{obs} . Back-extrapolation via this k_{obs} value indicates that in the initial reaction period, below $t = 40$ s, where MAA monomer is present, DTBP decomposes at a faster rate (see the residuals in the lower part of Fig. 8 and see text).

tion of this system has been studied at 200 °C, 500 bar and initial peroxide and acid concentrations of 0.150 mol DTBP/kg heptane and 0.160 mol MAA/kg heptane, respectively. The polymerization reaction is spectroscopically monitored via the decay of the C=C stretching mode absorption of MAA monomer, between 1625 and 1650 cm^{-1} , and the DTBP decomposition is measured, as before, via the TB band. The spectroscopically determined concentrations are plotted (in arbitrary units) in Fig. 8.

There is a rapid decay of acid monomer absorption which demonstrates the high polymerization rate of MAA. After about 40 seconds MAA (monomer) is consumed. The kinetic analysis of the TB concentration vs. time data has been restricted to the period after complete MAA consumption, that is for $t > 40$ s (open circles in Fig. 8). The first-order rate coefficient

found from this data, $k_{\text{obs}} = 2.1 \cdot 10^{-2} \text{ s}^{-1}$, is in full agreement with $k_{\text{HE}} = k_{\text{obs}}$ at $c_{\text{PA}} = 0$ in Table 1. As can be seen from the residuals in the lower part, the first-order rate law within the time interval 40 s to 300 s provides an excellent fit of the data. The rate coefficient for this interval, $k_{\text{obs}} = 2.1 \cdot 10^{-2} \text{ s}^{-1}$, may be used to extrapolate the TB concentration data back into the early reaction period, below 40 s, where MAA monomer is present. Subtraction of back-extrapolated TB concentrations from the measured ones (full circles in Fig. 8) yields significant differences. The residuals are clearly off zero. The deviation is such that during this time interval, in the presence of MAA, TB decays at an increased rate as compared to k_{obs} measured at $t > 40$ s. The important message from Fig. 8 is: Monomeric MAA increases DTBP decomposition rate, as does PA, whereas MAA segments within the polymer seem to be ineffective with regard to acid-induced decomposition. Although the total amount of acid groups remains constant, k_{obs} in the absence of monomeric MAA is the same as for DTBP decomposing in (pure) *n*-heptane.

Concerning high-pressure high-temperature ethene-MAA copolymerizations initiated by DTBP, the message from Fig. 8 is that, in addition to acid-induced DTBP decomposition being rather ineffective at high temperature, the influence of acid is further reduced as only monomeric MAA contributes to this rate enhancement. These aspects will be investigated in more detail directly during ethene-MAA copolymerizations [19]. Another interesting point originating from the present study relates to the possibility of tuning initiator decomposition rate in free-radical polymerization by adding small amounts of carboxylic acid. Studies along these lines are underway for the ethene high-pressure polymerization initiated by DTBP and tuned by acetic acid [19].

Acknowledgements

This work was carried out within the realm of the SFB 357 "Molekulare Mechanismen unimolekularer Reaktionen". The cooperation enjoyed with AKZO NOBEL (Research Center Deventer), in particular with Dr. B. Fischer, Dr. J. Meijer and Mr. R. Gerritsen is gratefully acknowledged, as is the discussion of experimental results and the support in GC analysis by that firm. We are also grateful for the interaction with BASF AG (Ludwigshafen), in particular with Dr. R. Klimesch, and for ethene being provided by BASF AG. L. W. is indebted to the "Stiftung Stipendien-Fonds des Verbandes der Chemischen Industrie e. V." and to the BMBF for financial support.

References

1. A. Rudin, *The Elements of Polymer Science and Engineering*, Academic Press, Orlando (1982).

2. J. C. Masson, in *Polymer Handbook*, 3rd edition, eds. J. Bandrup and E. H. Immergut, John Wiley and Sons, New York, (1989).
3. M. Buback and C. Hinton, *Z. Physik. Chem.* **193** (1996) 61.
4. S. Klingbeil, *Ph. D. Thesis*, Göttingen (1995).
5. M. Buback and C. Hinton, *Z. Physik. Chem.* **199** (1997) 229.
6. P. D. Bartlett and J. E. Leffler, *J. Am. Chem. Soc.* **72** (1950) 3030.
7. A. T. Blomquist and A. F. Ferris, *J. Am. Chem. Soc.* **73** (1951) 3912.
8. H. Hart and R. A. Cipriani, *J. Am. Chem. Soc.* **84** (1962) 3697.
9. J. E. Leffler and C. C. Petropoulos, *J. Am. Chem. Soc.* **79** (1957) 3068.
10. E. S. Huyser and R. M. Van Scoy, *J. Org. Chem.* **77** (1968) 3524.
11. A. Drefahl, *Diploma Thesis*, Göttingen (1984).
12. M. Buback and H. Lendle, *Z. Naturforsch.* **34a** (1979) 1482.
13. T. Koenig, in *Free Radicals*, Vol. 1, ed. J. K. Kochi, John Wiley and Sons, New York (1973) 113.
14. T. Koenig and H. Fischer, in *Free Radicals*, Vol. 1, ed. J. K. Kochi, John Wiley and Sons, New York (1973) 157.
15. G. Luft, P. Mehrling and H. Seidl, *Angew. Makromol. Chem.* **73** (1978) 95.
16. C. Walling and H. P. Waits, *J. Phys. Chem.* **71** (1967) 2361.
17. H. Kiefer and T. G. Traylor, *J. Am. Chem. Soc.* **89** (1967) 6667.
18. R. N. Neuman, Jr., and R. J. Bussey, *J. Am. Chem. Soc.* **92** (1970) 2440.
19. L. Wittkowski, *Ph. D. Thesis*, Göttingen (1998).
20. A. van Herk, *J. Chem. Ed.* **72** (1995) 138.
21. M. Buback, K. Gerke, C. Ott, and L. F. Tietze, *Chem. Ber.* **127** (1994) 2241.
22. E. M. Borschel and M. Buback, *Z. Naturforsch.* **42a** (1987) 187.